Solitons in the midst of chaos

Vlad Seghete and Curtis R. Menyuk
Department of Computer Science and Electrical Engineering, University of Maryland Baltimore County, 1000 Hilltop Circle, Baltimore, Maryland 21250, USA

Brian S. Marks
Department of Statistics and Department of Psychological and Brain Sciences, 1101 East 10th Street, PY 190A, Bloomington, Indiana 47405, USA

(Received 31 January 2007; published 5 October 2007)

A system of coupled nonlinear Schrödinger equations describes pulse propagation in weakly birefringent optical fibers. Soliton solutions of this system are found numerically through the shooting method. We employ Poincaré surface of section plots—a standard dynamical systems approach—to analyze the phase space behavior of these solutions and neighboring trajectories. Chaotic behavior around the solitons is apparent and suggests dynamical instability. A Lyapunov stability analysis confirms this result. Thus, solitons exist in the midst of chaos.

DOI: 10.1103/PhysRevA.76.043803 PACS number(s): 42.81.Dp, 05.45.Yv, 42.25.Lc

I. INTRODUCTION

Solitons [1,2] propagating through optical fibers [3] have received a large amount of attention due both to their interesting mathematical properties and their potential uses in optical fiber technology. Solitons are solitary waves that achieve a balance between linear dispersive effects and nonlinear effects in such a way that they maintain their shape over long distances. This interesting behavior has suggested the use of solitons as information carriers in optical fibers or as mode-locked laser pulses [3]. A large amount of research has been performed in order to understand the nature of these solitons. Pulse propagation through an optical fiber is described by the nonlinear Schrödinger equation

$$iu_z + \frac{1}{2}u_{tt} + |u|^2 u = 0, \tag{1}$$

where u is the complex envelope of the electric field, t is the retarded time, and z is the propagation distance along the optical fiber. The subscript z indicates a derivative with respect to distance z and the subscript t indicates a derivative with respect to time t. We have used soliton normalization to remove the explicit dependence on the dispersion coefficient and nonlinear coefficient [3]. Equation (1) is solvable through the inverse scattering transform and detailed descriptions of this method of solution can be found in Refs. [1,2].

While our study was motivated by this equation's application to optical fibers, we note that the nonlinear Schrödinger equation applies to a wide variety of physical systems [1,2], and our results—which make no appeal to the particular properties of optical fibers or, for that matter, to any optical system—have an equally broad range of applicability. The solutions of the nonlinear Schrödinger equation accurately describe the propagation of pulses through single-mode fibers, but in reality most optical fibers are not single mode, and the pulses that propagate in them are affected by birefringence due to fiber imperfections. Birefringence can cause pulses to split, as one polarization mode lags behind the other. The propagation of these two polarization modes is often described by a system of coupled nonlinear Schrödinger equations

$$iu_z + \frac{1}{2}u_{tt} + (|u|^2 + \beta|v|^2)u = 0, \tag{2a}$$

$$iv_z + \frac{1}{2}v_{tt} + (\beta|u|^2 + |v|^2)v = 0, \tag{2b}$$

where u and v are normalized complex envelopes of the two polarizations and β is the nonlinear coupling strength. In birefringent optical fibers, β varies from $2/3$ to 2 depending on the ellipticity of the polarization states [4]. Again, while our work on this system was motivated by applications to birefringent optical fibers, we note that this equation applies generically to physical systems in which two modes are coupled through a cubic interaction [1,2].

In the context of optical fibers, Eq. (2) is more fundamental than the nonlinear Schrödinger equation. The nonlinear Schrödinger equation can be derived from it assuming that a single polarization state is launched into the fiber and the light remains in a single polarization state as a function of time at any distance z along the fiber, although this state can (and typically does) change as a function of z. Given this equation's importance in optical fiber applications it has been the subject of a large amount of work. Its soliton solutions, in particular, have been studied using a combination of analytical and numerical techniques, including perturbation theory and the shooting method [5–8].

Despite all this work, important fundamental questions concerning the soliton solutions to Eq. (2) remain unanswered. Equation (1) is an integrable system that can be solved using the inverse scattering transform technique. An important consequence is that it has soliton solutions that are stable in the sense that permanent solitary wave solutions exist that propagate indefinitely. These soliton solutions are such that $|u(z,t)|^2$ only depends on the variable combination $t-\alpha z$, where α is a group velocity parameter, rather than on

t and z separately. The parameter α may always be made zero by a translation of t and the phase of u. Hence, we may refer to these solutions as stationary. This soliton solution is one member of a family of stationary solutions, each of which consists of a periodic train of pulses such as would emerge from a passively mode-locked laser [3]. A second, important sense in which the soliton solutions of Eq. (1) are stable is that they are embedded in a family of stationary solutions, all of which have a fixed periodicity.

By contrast, Eq. (2) is not integrable except in the special cases $\beta=0$ and $\beta=1$ or when the initial conditions are suitably restricted [9]. As a consequence, it has chaotic solutions [9]. Under these circumstances, one might question whether permanent soliton solutions exist at all. If we consider, for example, a perturbed version of the nonlinear Schrödinger equation

$$iu_z + \frac{1}{2}u_{tt} + i\epsilon u_{ttt} + |u|^2 u = 0, \tag{3}$$

where ϵ is a small parameter, then it is possible to construct a soliton solution to Eq. (3) to all powers in ϵ. Moreover, computational results show a sharp threshold in ϵ below which there is no sign of instability. Nonetheless, Wai *et al.* [10] have shown that this soliton radiates "beyond all orders" and there is, strictly speaking, no permanent soliton solution.

Yang [8] has found soliton solutions to Eq. (2) using the shooting method and has demonstrated that they are stable when β is sufficiently close to 0 or 1 in the sense that they are permanent solitons, such as the soliton solution to Eq. (1). One purpose of this paper is to demonstrate for nontrivial β ($\beta=2/3$) in one important instance that the soliton solutions found by the shooting method are in fact stable in the sense that they are permanent solitons. We will also elucidate the physical reasons that this stability is expected to be generic.

The second purpose of the paper is to demonstrate that these solitions are not stable in the sense that they are embedded in a family of chaotic stationary solutions. These chaotic solutions come arbitrarily close to the soliton solutions in a well-defined phase space. Thus, we may truly say that these solitons exist in the midst of chaos.

The remainder of this paper is organized as follows. In Sec. II we review the theory of stationary solutions to Eq. (1) in a form that will be of use in the remainder of the paper. In Sec. III, we derive the ordinary differential equations that govern the stationary solutions and describe some of their properties. In Sec. IV we show how to obtain soliton solutions using the shooting method and demonstrate in one nontrivial instance that this solution is a permanent soliton. We discuss the physical reasons that the stability is expected to be generic. In Sec. V we use surface of section plots to demonstrate the existence of chaos in the neighborhood of solitons, and we demonstrate that the Lyapunov exponent associated with the soliton solutions is nonzero. Section VI contains the conclusions.

II. SOLITON SOLUTIONS TO THE NONLINEAR SCHRÖDINGER EQUATION

We are interested in solutions to Eq. (1) in the form

$$u(z,t) = f(t-\alpha z)\exp(-i\omega t + ikz). \tag{4}$$

These solutions are the simplest in a large family of quasiperiodic solutions to the nonlinear Schrödinger equation [11]. We first note that any such solution may be translated into a solution of the form

$$u(z,t) = f(t)\exp(ikz), \tag{5}$$

and hence it is sufficient to consider solutions in the latter form. The equivalence of the two solution forms is supported by the transformation

$$\zeta = \frac{\omega}{k}t + z, \quad \tau = t - \alpha z. \tag{6}$$

This change of variables does not change the partial derivatives of u with respect to t and z,

$$u_{tt} = u_{\tau\tau}, \quad u_z = u_\zeta, \tag{7}$$

which satisfies Eq. (1) in the new variables. Hence, going back to the old notation, we can simplify the problem by just looking at solutions of the form shown in Eq. (5).

Substituting Eq. (5) into Eq. (1) we obtain

$$-kf + \frac{1}{2}f_{tt} + f^3 = 0, \tag{8}$$

where $f=f(t)$ is the z-independent envelope of $u(z,t)$. Integrating the previous equation we have

$$H = -kf^2 + \frac{1}{2}f_t^2 + \frac{1}{2}f^4, \tag{9}$$

with H a suitably chosen constant of integration. We will use H as the Hamiltonian of a dynamical system described by Eq. (8). To make the Hamiltonian structure clear, we denote

$$q = f, \quad p = f_t, \tag{10}$$

where q and p are the generalized coordinate and momentum of our system. In the new notation H verifies Hamilton's equations so that Eq. (9) defines H as the Hamiltonian of a dynamical system with

$$q_t = p, \tag{11a}$$

$$p_t = 2kq - 2q^3, \tag{11b}$$

$$H = \frac{1}{2}q^4 - kq^2 + \frac{1}{2}p^2. \tag{11c}$$

We are looking for real solutions of this system, and hence values of H for which both q and p exist and are real. We rewrite Eq. (11c) as

$$H = F(q,k) + \frac{1}{2}p^2. \tag{12}$$

Figure 1 shows $F(q)$ for $k>0$. We will only present this case, since the case $k<0$ is practically equivalent to the case in which $H>0$, as presented below. As we can see there are

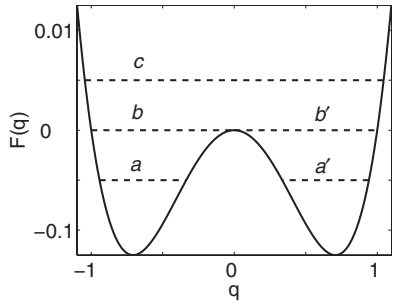

FIG. 1. The graph of $F(q)$ from Eq. (12) shown at $k=1/2$. The dotted horizontal lines correspond to different values of H, each of them illustrating a different region of similar solutions to Eq. (9): a and a' correspond to $H\in[-k^2/2,0)$, b and b' correspond to $H=0$, and c corresponds to $H>0$.

three separate cases in which real solutions to the Hamiltonian system in Eq. (11) exist, corresponding to $0>H>-k^2/2$, $H>0$, and $H=0$. The equation

$$q_t^2 = 2H + 2kq^2 - q^4, \tag{13}$$

which is simply a restatement of Eq. (9), can be solved in terms of Jacobi elliptic functions [12] to yield the solutions

$$q = \pm A\,\mathrm{dn}(At|m_1), \tag{14a}$$

$$q = \pm A\,\mathrm{sech}(At), \tag{14b}$$

$$q = A\,\mathrm{cn}(\sqrt{2}(k^2+2H)^{1/4}t|m_2), \tag{14c}$$

where we have used

$$A = (k+\sqrt{k^2+2H})^{1/2}, \tag{15a}$$

$$m_1 = \frac{2\sqrt{k^2+2H}}{A^2}, \tag{15b}$$

$$m_2 = \frac{A^2}{2\sqrt{k^2+2H}}. \tag{15c}$$

The solutions in Eqs. (14a)–(14c) correspond to the three cases mentioned above, $0>H>-k^2/2$, $H>0$, and $H=0$, respectively, as can be seen from Fig. 1. The solution in Eq. (14c) can be obtained by setting $H=0$ in the other two solutions. This solution is of particular interest to us, since it represents the soliton solution of the equation. For reasons that will become evident later, we present in Fig. 2 the phase space profile for the dynamical system defined by Eq. (11). Note that the soliton solutions lie on homoclinic trajectories, separating the solutions presented in Eq. (14a) from the solutions presented in Eq. (14c). Figures 3(a)–3(c) show the same trajectories plotted in the time domain.

As a conclusion to this section we note that we found soliton solutions to Eq. (1) in the form

$$u(z,t) = \pm A\,\mathrm{sech}(At)\exp\left(i\frac{A^2}{2}z\right). \tag{16}$$

We also noted the special role played by the soliton solutions as separatrices in the phase space of our dynamical system.

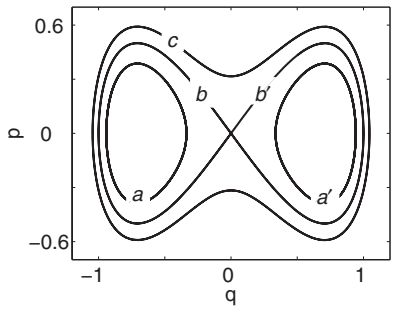

FIG. 2. A phase space diagram of the system in Eq. (11) with trajectories corresponding to the values of the Hamiltonian presented in Fig. 1: a and a' correspond to $H\in[-k^2/2,0)$, b and b' correspond to $H=0$, and c corresponds to $H>0$. The actual values are $H=-0.05$, $H=0$, and $H=0.05$. A time domain representation of the solutions corresponding to the trajectories can be seen in Fig. 3.

III. BIREFRINGENT FIBER EQUATIONS

As shown in previous works [5,13] light propagation through a birefringent optical fiber is governed by two coupled nonlinear Schrödinger equations, presented in Eq. (2), with z and t the normalized distance and time [5]. When $\beta=0$ the two equations decouple into two separate one-dimensional nonlinear Schrödinger equations, each of them analytically integrable with soliton solutions. This case corresponds to the absence of birefringence. Also, for the case $\beta=1$, Manakov [14] showed that the system is integrable by using the inverse scattering method and found a whole family of solutions. Numerical work and Painlevé analysis indicate that these are the only values of β that yield an integrable system [15].

For practical purposes, however, it is useful to understand the behavior of these equations for other values of β. In these cases numerical methods prove useful in determining the existence of soliton solutions and their nature. To integrate the equations numerically we consider solutions of the form

$$u(z,t) = f(t)\exp(ik_1 z), \tag{17a}$$

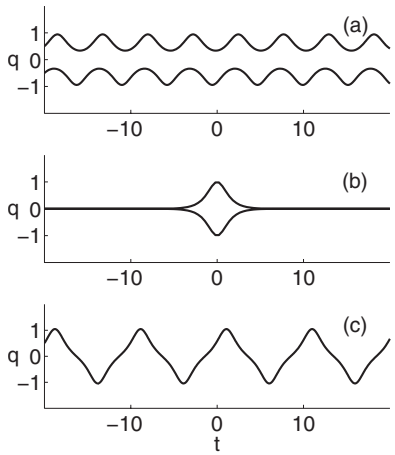

FIG. 3. The time domain representation of several solutions of Eq. (11), corresponding to the phase space trajectories shown in Fig. 2. The same numerical values are used. Note that the soliton solution in (b) corresponds to a homoclinic trajectory in Fig. 2.

$$v(z,t) = g(t)\exp(ik_2 z), \tag{17b}$$

where f and g are two real functions, and k_1 and k_2 are two real parameters. Substituting Eq. (17) into Eq. (2), we obtain

$$f_{tt} - 2k_1 f + 2(f^2 + \beta g^2)f = 0, \tag{18a}$$

$$g_{tt} - 2k_2 g + 2(g^2 + \beta f^2)g = 0. \tag{18b}$$

In order to have solutions decaying as $t \to \pm\infty$, the parameters k_1 and k_2 must be positive. Also, it is not necessary to investigate all possible combinations of k_1 and k_2, as a simple scaling from t to $t/\sqrt{k_1}$ shows that we can set $k_1 = 1$ without any loss of generality [8].

In order to numerically integrate the system, it is useful to transform Eq. (18) from second order to first order ODEs. We close by considering the two functions f and g and their derivatives f_t and g_t as generalized coordinates and momenta in a dynamical system

$$q_1 = f, \quad p_1 = f_t, \quad q_2 = g, \quad p_2 = g_t, \tag{19}$$

where q_1, p_1, q_2, and p_2 are the generalized coordinates and momenta. The notational transformation in Eq. (19) leads to the Hamiltonian

$$H = \frac{1}{2}p_1^2 + \frac{1}{2}p_2^2 - k_1 q_1^2 + \frac{1}{2}q_1^4 + \beta q_1^2 q_2^2 - k_2 q_2^2 + \frac{1}{2}q_2^4, \tag{20}$$

and thus Hamilton's equations of this system are

$$q_{1t} = p_1, \tag{21a}$$

$$q_{2t} = p_2, \tag{21b}$$

$$p_{1t} = 2k_1 q_1 - 2(q_1^2 + \beta q_2^2)q_1, \tag{21c}$$

$$p_{2t} = 2k_2 q_2 - 2(\beta q_1^2 + q_2^2)q_2. \tag{21d}$$

If we impose the condition that solutions decay at infinity (pulse solutions), the Hamiltonian of the system must equal zero,

$$H = 0. \tag{22}$$

This observation is important, as our focus is the soliton solutions, and we will therefore only analyze systems with $H=0$. Also, in all the computations presented here we chose the value $\beta = 2/3$, since it is of importance in birefringent optical fibers. Very similar results are found for all other values of β in the range $(0,1)$ that we investigated.

At the same time, we note that almost all solutions that we will be finding, even though $H=0$, do not decay to zero as $t \to \pm\infty$. As a consequence, the instability of the soliton solutions that we will observe cannot in general be used to infer that Eq. (2) will be unstable once boundary conditions such as $u(z,t) \to 0$ as $t \to \pm\infty$ are imposed. Different methods must be used for that purpose [1,2].

IV. EXISTENCE OF SOLITON SOLUTIONS

Before starting the search for numerical soliton solutions to Eq. (21) we should ensure that these solutions exist. What follows is an argument that shows that at least one class of these solutions does indeed exist and also gives useful information about the algorithm to find them.

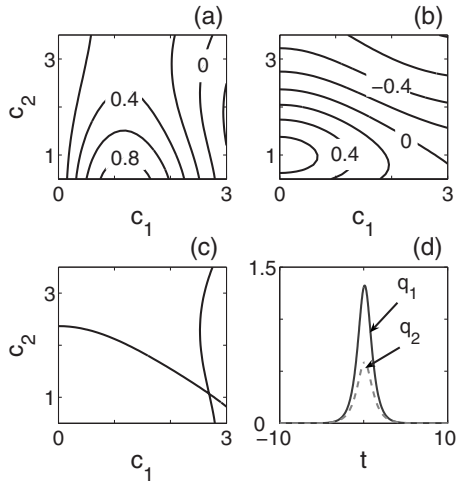

FIG. 4. Argument for the existence of a symmetric soliton solution to the coupled nonlinear Schrödinger equation in the case $k_1=1$, $k_2=0.7$, and $\beta=2/3$. (a) Contour plot of the difference between $p_1(t=0,c_1,c_2)$ when integrating from the left and its value when integrating from the right based on initial asymptotic coefficient pairs for the first normal mode; (b) similar contour plot for the second normal mode; (c) zero-level contours for both normal modes, with an intersection at $c_1=2.69$ and $c_2=1.07$; (d) the soliton corresponding to the initial conditions in (c).

One class of solutions we will be looking for is symmetric pulses. These are the simplest to describe since the only condition is that the generalized momenta vanish simultaneously at $t=0$. If this holds true, then it follows from the symmetry of Eq. (21) that the solution will be symmetrical with respect to the $t=0$ axis. As we have discussed in the previous section, we are interested in solutions that vanish as $t \to \pm\infty$. Let us consider $t \to -\infty$ and impose that q_1 and q_2 vanish in this limit. We then find that the nonlinear terms in Eq. (21) disappear and the resulting solutions as $t \to -\infty$ must satisfy

$$q_1(t) \to c_1 \exp(\sqrt{2k_1}t), \tag{23a}$$

$$q_2(t) \to c_2 \exp(\sqrt{2k_2}t), \tag{23b}$$

where c_1 and c_2 are constants. Our goal is to find c_1 and c_2, such that the solution to Eq. (21) yields $p_1(0)=0$ and $p_2(0)=0$. If such c_1 and c_2 exist, then we will have shown that Eq. (21) has a soliton solution that is symmetric about $t=0$.

To determine c_1 and c_2, we consider the contour plots of the functions $p_1(t=0,c_1,c_2)$ and $p_2(t=0,c_1,c_2)$, shown in Figs. 4(a) and 4(b). The plots were obtained numerically using an adaptive step-size fifth order Runge-Kutta method, starting at $t=-10$ and integrating toward zero with the initial conditions from Eq. (23). The parameter values are $k_1=1$, $k_2=0.7$, and $\beta=2/3$. We see in Fig. 4(c) that the curves for $p_1(0)=0$ and $p_2(0)=0$ intersect, so that there indeed exists a pair of values of c_1 and c_2 that will generate a symmetric soliton. To find the numerical values of the zero crossing of p_1 and p_2 we use a shooting method in which we search for

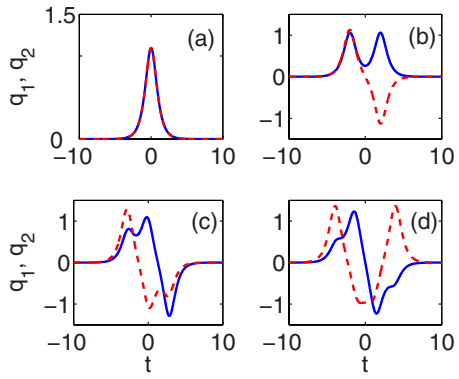

FIG. 5. (Color online) Numerical solutions with $\beta=2/3$, $k_1=k_2=1$. The solid and the dashed curves represent q_1 and q_2, respectively, plotted vs the normalized time t.

zeros of $p_1^2+p_2^2$ as a function of c_1 and c_2. This argument can be extended to cases that are not symmetric about $t=0$ by using a different function of the two variables and applying an appropriate zero-finding algorithm.

In this case, the shooting method consists of picking two initial points, one at a negative t value and one at a positive t value. Integrating both toward zero we obtain two different sets of values for the variables at $t=0$. We then consider the difference in these final values as a function of the initial conditions. Applying a Newton-Raphson minimization algorithm on the resulting difference, combined with a good initial guess, will result in a convergent solution of the system of equations. In order to find the soliton solutions, it is useful to impose that the starting points comply with the asymptotic relations for large $|t|$, not unlike in the previous existence argument

$$p_1 = \sqrt{2k_1}q_1, \tag{24a}$$

$$p_2 = \sqrt{2k_2}q_2. \tag{24b}$$

The relations in Eq. (24) are a consequence of the soliton's exponential decay at $t \to \pm\infty$. Figures 5 and 6 illustrate several soliton solutions found through this method for different values of k_2. The solid curves represent q_1 while the dotted curves represent q_2.

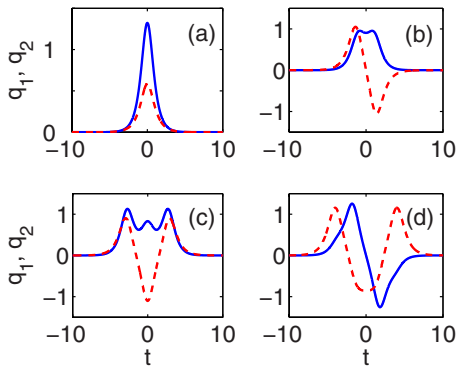

FIG. 6. (Color online) Numerical solutions with $\beta=2/3$, $k_1=1$, $k_2=0.7$. The solid curve represents q_1 and the dashed curve represents q_2.

Figure 5(a) shows a soliton solution in which the two modes are equal, for $\beta=2/3$ and $k_1=k_2=1$. These solutions can be found analytically, and may be written

$$q_1 = q_2 = \left(\frac{2}{1+\beta}\right)^{1/2} \operatorname{sech}\sqrt{2}t, \tag{25}$$

which is in agreement with the numerical results. All other cases that we found do not correspond to known analytical solutions, although the solution shown in Fig. 6(a) can be analytically approximated by a daughter-wave solution, as shown by Yang [6].

The validity—and, in one sense, the stability—of the solutions yielded by the shooting method is supported by the existence of solutions. The convergence of the Newton-Raphson algorithm in certain regions, for multiple initial values in those regions, is a strong indication that our solutions are valid, since we only deal with continuous functions. Moreover, since the initial approximation in Eq. (24) was such that we only look for soliton solutions, all instances in which the algorithm converges correspond to an approximation of a soliton.

Concerning the permanence of such solutions it is useful to first look at the solutions of Eq. (1). The soliton solution to this equation is shown in Eq. (16), and its dispersion relation is given by $k_{\text{sol}}=A^2/2$. The dispersion relation for the linear wave solutions of Eq. (1) is found by substituting $\exp(ik_{\text{lin}}z - i\omega t)$ into Eq. (1) and ignoring the nonlinear term. We obtain $k_{\text{lin}}=-\omega^2/2$, which implies that it will always be the case that $k_{\text{lin}}<0$ while $k_{\text{sol}}>0$. As a consequence the soliton will never be in resonance with linear dispersive waves and energy will not be permanently transferred between the two. This is the physical reason that a permanent soliton exists. This situation is in contrast with that of Eq. (3) where the linear dispersion relation is

$$k_{\text{lin}} = -\frac{1}{2}\omega^2 - \epsilon\omega^3, \tag{26}$$

and for any value of k there is always an ω such that $k=k_{\text{lin}}$ [15]. Thus, there is always a frequency at which linear dispersive waves will resonate with the soliton, resulting in radiation "beyond all orders" [10,16]. This reasoning is purely heuristic and no replacement for a direct demonstration of either stability or radiation "beyond all orders." However, it appears to work well in practice and provides physical insight.

We may apply a similar heuristic reasoning to the solutions of Eq. (2). The linear dispersion relations for Eq. (2) are

$$k_{1\text{lin}} = k_{2\text{lin}} = -\frac{1}{2}\omega^2, \tag{27}$$

and the wave numbers are always negative. Soliton solutions of Eq. (2), are expected to have wave numbers $k_{1,2}>0$. For example, if we look at the soliton solution in Eq. (25), its dispersion relation is

$$k_{1\mathrm{sol}} = k_{2\mathrm{sol}} = (\beta + 1)\frac{A^2}{2}, \tag{28}$$

so that $k_{\mathrm{sol}} > 0$ whenever $\beta > -1$. Yang [8] looked at this solution in more detail, and found that soliton solutions are permanent for positive values of β. He also presents several other classes of solutions for which a very similar physical argument indicates stability. The shooting method that we use assumes $k_1 > 0$ and $k_2 > 0$ [see Eqs. (23) and (24)] and thus can only find solutions that satisfy this condition. Thus, it is reasonable to conclude that soliton solutions are stable in the sense that they are permanent and do not radiate "beyond all orders."

V. SURFACE OF SECTION PLOTS

In order to better understand the existence and evolution of the soliton solutions of Eq. (2), we analyze the phase space of the Hamiltonian system in Eq. (20). Using the analog of the one-dimensional system discussed in Sec. II, we expect to find solitons as separatrices between different types of oscillatory solutions. Using the adaptive step-size fifth order Runge-Kutta method we integrate Eq. (21) from several starting points, including the ones corresponding to the soliton solutions found previously by the shooting method.

When integrating Eq. (21) numerically, we fix $H=0$ in order to obtain soliton solutions, as mentioned previously. Hence, one of the variables becomes a function of the other three. The result is a trajectory that lies on a three-dimensional energy surface in a four-dimensional phase space. Representing the curve in the four-dimensional space would be confusing and hard to interpret. To solve this problem we look at sections through the space, which render two-dimensional figures that are easier to generate and interpret, called Poincaré surfaces of section [18]. To obtain such a section we start integrating Eq. (21) forward in time from a particular initial point. Every time q_2 reaches a certain chosen value Q with $p_2 > 0$, we plot the values of q_1 and p_1, ignoring p_2. We thus obtain a section of the phase space, rendering an image similar to a two-dimensional phase plot. The value of the initial p_2 was computed from Eq. (20) imposing the condition $H=0$.

The boundaries of the space are found from Eq. (20) with the observation that, in order to maximize p_1, we have to take $p_2=0$. The boundary is then given by

$$p_1 = \sqrt{\delta}\sin\tau, \tag{29a}$$

$$q_1 = \pm(\sqrt{\delta}\cos\tau + \gamma)^{1/2}, \tag{29b}$$

$$\tau \in [-\arccos(-\gamma/\sqrt{\delta}), \arccos(-\gamma/\sqrt{\delta})], \tag{29c}$$

where

$$\delta = (\beta^2 - 1)Q^4 + 2Q^2(k_2 - k_1\beta) + k_1^2, \tag{30a}$$

$$\gamma = k_1 - \beta Q^2. \tag{30b}$$

The parameters δ and γ are constants, dependent on the equation parameters and the value at which the section is taken. Thus, we cannot take such a section at a value of Q that will generate a negative δ. Such a choice of Q would be outside of the phase space of the problem.

In Figs. 7(a) and 8 we present two surfaces of section. We again set $\beta=2/3$. Results for other values of β are similar qualitatively except for the integrable cases $\beta=0$ and $\beta=1$ [14]. The marked points represent the solitons determined in Figs. 5 and 6. Since these solutions decay as $t \to \pm\infty$, they do not intersect the plane at more than a small number of points. However, all other points on the plots are found by integrating trajectories that are close to the solitons. Figures 7(b)–7(d) are magnified to show more detail around the intersections of the soliton solitions with the surfaces of section. What is remarkable is that every soliton is surrounded by chaotic regions. Each soliton is, in fact, placed at an intersection of boundaries of chaos, as shown in Fig. 7(b). In this case the thickness of the chaotic regions is small compared to the dimension of the phase space, and the behavior of the trajectories seems to indicate that proximity to a soliton trajectory implies instability. A trajectory will follow a regular path for a long time far away from the soliton trajectory, but when it eventually comes close to it in phase space the strong instability pushes it away, thus generating the chaotic pattern seen in Figs. 7(c) and 7(d). This can be understood intuitively when compared to the homoclinic trajectories in the phase space of the Hamiltonian of Eq. (1). The solitons in this case act as bridges between different regions of chaotic behavior. In Fig. 8, which corresponds to $k_1 \neq k_2$, we can see the chaotic behavior even without any magnification. The solitons in this case exist in the midst of chaos. The thickness of the chaotic region suggests a higher degree of instability of these solutions than of the previous ones. We proceed by quantitatively determining this difference through a linear stability analysis.

In order to confirm that the regions surrounding these soliton trajectories are chaotic we performed a linear stability analysis of the numerical solutions we obtained with the shooting method. To do this we calculated the Lyapunov exponent [17] by integrating both the original solution and a nearby, perturbed trajectory; the average of the normalized perturbation over the time elapsed was plotted. We expect the Lyapunov exponents of unstable trajectories to level off while those of stable trajectories will tend to zero.

In Fig. 9 we show the Lyapunov exponents for the solitons solutions obtained in the previous section. For reference we have also plotted the result of our analysis on a soliton that is known to be stable from previous analytical investigation of the Manakov equations and also an oscillatory solution of Eq. (21). While the Lyapunov exponent of these latter solitons tends to zero, those of the solitons found in the case $\beta=2/3$ level off eventually, indicating that they are indeed surrounded by chaos and that small perturbations of the trajectories in these areas increase exponentially. Also, the Lyapunov exponents are lower in the case $k_1=k_2$ than in the case of distinct k_1 and k_2. This is consistent to our observation that the chaotic regions in the former system are thinner and more interspersed with isles of stability. The Lyapunov

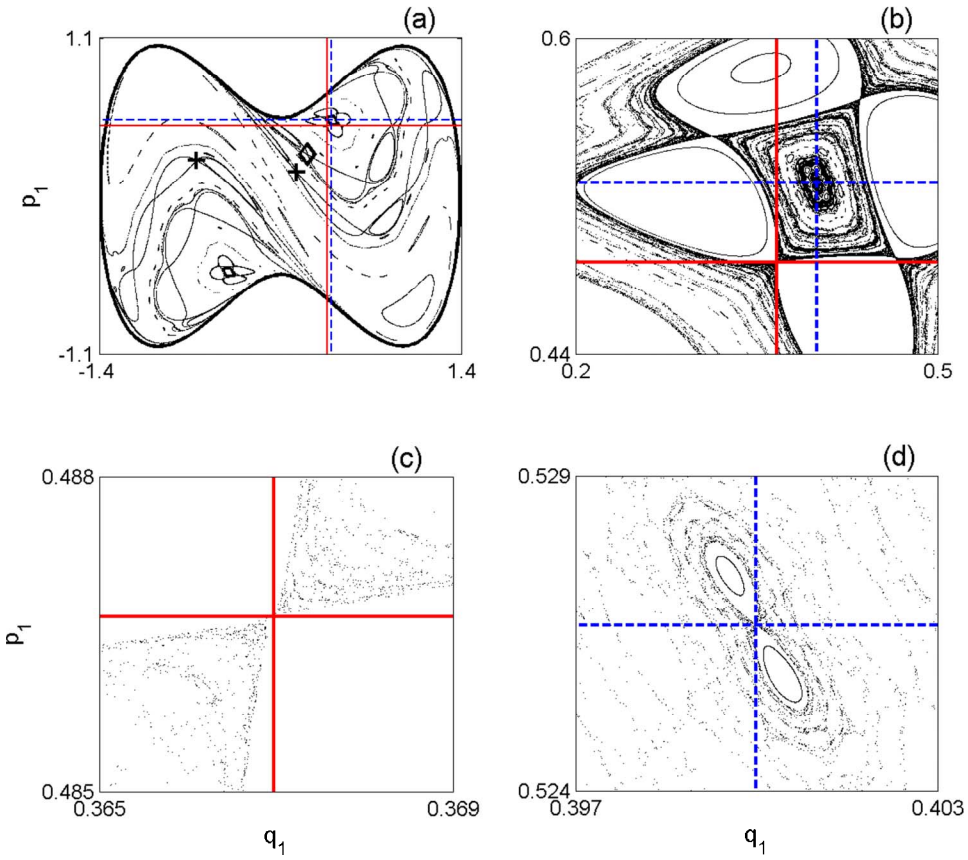

FIG. 7. (Color online) Surfaces of section taken at $q_2=0.4$ with $\beta=2/3$, $k_1=k_2=1$. (a) The entire phase space section is presented; (b) a magnification in the neighborhood of two of the soliton trajectories; (c) and (d) further magnifications with the soliton solution intersects in the middle of the figure. The solitons in (c) and (d) are placed at the intersection of the marker lines, dashed for the soliton in Fig. 5(a) and solid for the one in Fig. 5(b). The diamonds and the crosses in (a) mark the intersections of the solitons in Figs. 5(c) and 5(d), respectively.

exponents of all solitons in Fig. 5 tend to the same value, indicating that, just as in Fig. 8, all the chaotic regions surrounding the islands of stability in Fig. 7 are, in fact, one extended region of connected trajectories. However, due to the lesser degree of instability of this region it is harder to make this observation directly from the surface of section plots.

VI. CONCLUSION

In this paper we reduced the coupled nonlinear Schrödinger equations to a fourth order (two degree-of-freedom) Hamiltonian system using an ansatz that focused on stationary solutions of the original equations. We then applied standard dynamical methods to this reduced system. We showed that soliton solutions that decay exponentially as $t \to \pm\infty$ exist, and we found several of them through a shooting method and argued for their permanence. Thus, solitons are stable in the sense that they are permanent, rather than radiating "beyond all orders." Using Poincaré surfaces of section, we analyzed the dynamical behavior of the phase

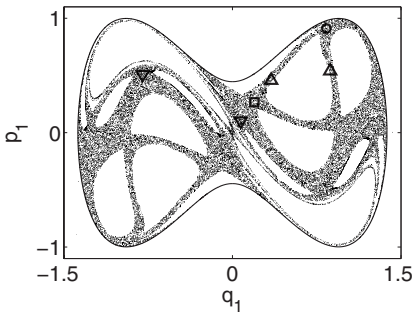

FIG. 8. Surface of section taken at $q_2=0.4$ with $\beta=2/3$, $k_1=1$, and $k_2=0.7$. The soliton intersections represented by a circle, rectangle, upper triangles and lower triangles correspond to Figs. 6(a), 6(b), 6(c), and 6(d) respectively. They are located in the same region of visible chaos.

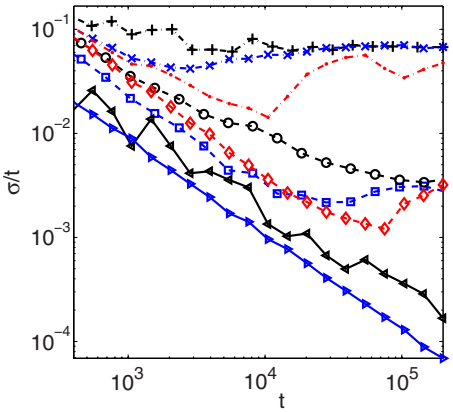

FIG. 9. (Color online) Linear stability analysis showing average normalized deviation vs time. The dotted lines correspond to solitons in the $k_1 \neq k_2$ case (Fig. 6) and the dashed lines to solitons in the $k_1=k_2=1$ case, as in Fig. 5; the solid lines represent a soliton solution of the Manakov system [14] (triangles pointing left) and a regular oscillatory solution of the $\beta=2/3$, $k_1=k_2=1$ system (triangles pointing right).

space in which these solitons exist. We found that, when $\beta = 2/3$, the solitons are surrounded by chaotic regions. Thus, the soliton solutions resemble the homoclinic trajectories that are found in the second order Hamiltonian system (one degree-of-freedom). A Lyapunov stability analysis showed that soliton solutions to the coupled nonlinear Schrödinger equations are unstable in the dynamical sense. We conclude that although permanent soliton solutions to the coupled nonlinear Schrödinger equations exist for nonintegrable cases, they exist in the midst of chaos.

ACKNOWLEDGMENTS

V. S. is grateful for support from UMBC. It is a pleasure to acknowledge useful discussions with Professor Jianke Yang of the University of Vermont.

[1] P. G. Drazin and R. S. Johnson, *Solitons: An Introduction (Cambridge Texts in Applied Mathematics)* (Cambridge University Press, Cambridge, 1989).
[2] M. J. Ablowitz and H. Segur, *Solitons and the Inverse Scattering Transform* (SIAM, Philadelphia, 1981).
[3] A. Hasegawa and Y. Kodama, *Solitons in Optical Communications* (Oxford University Press, Oxford, United Kingdom, 1995).
[4] C. R. Menyuk, IEEE J. Quantum Electron. **QE-25**, 2674 (1989).
[5] C. R. Menyuk, IEEE J. Quantum Electron. **QE-23**, 174 (1987).
[6] J. Yang, Physica D **108**, 92 (1997).
[7] J. Yang, Stud. Appl. Math. **97**, 127 (1996).
[8] J. Yang and D. J. Benney, Stud. Appl. Math. **96**, 111 (1996).
[9] G. Baumann, W. G. Glockle, and T. F. Nonnenmacher, Proc. R. Soc. London, Ser. A **434**, 263 (1991).
[10] P. K. A. Wai, H. H. Chen, and Y. C. Lee, Phys. Rev. A **41**, 426 (1990).
[11] E. R. Tracy and H. H. Chen, Phys. Rev. A **37**, 815 (1988), and references cited therein.
[12] M. Abramowitz and I. A. Stegun, *Handbook of Mathematical Functions* (Dover Publications, Inc., New York, 1970).
[13] D. J. Benney and A. C. Newell, J. Math. Phys. (Cambridge, Mass.) **46**, 133 (1967).
[14] S. V. Manakov, Sov. Phys. JETP **38**, 248 (1974).
[15] R. Sahadevan, K. M. Tamizhmani, and M. Lakshmanan, J. Phys. A **19**, 1783 (1986).
[16] N. Akhmediev and M. Karlsson, Phys. Rev. A **51**, 2602 (1995).
[17] A. J. Lichtenberg and M. A. Lieberman, *Regular and Chaotic Dynamics* (Springer-Verlag, New York, 1992), pp. 2429.
[18] A. J. Lichtenberg and M. A. Lieberman, *Regular and Chaotic Dynamics* (Springer-Verlag, New York, 1992), pp. 1220.